Article Pre-Print

Actuator and Sensor Fault Isolation of Solution Copolymerization of MMA and VAc Process

Hadi Shahnazari and Prashant Mhaskar*

Department of Chemical Engineering, McMaster University

Hamilton, ON L8S 4L7 Canada

* Corresponding author's e-mail address: mhaskar@mcmaster.ca

Abstract

In this work, we consider the problem of isolating actuator and sensor faults in the solution copolymerization of Methyl Methacrylate (MMA) and Vinyl Acetate (VAc) monomers. To this end, first a bank of high gain observers are designed, and fault-detection and isolation (FDI) residuals are defined. The process dynamics are further analyzed to categorize fault scenarios as distinguishable and indistinguishable, and the necessary and sufficient conditions for the classification are presented. Subsequently, filters are designed that enable FDI for the distinguishable fault scenarios and fault detection for the indistinguishable fault scenarios. The FDI filters are implemented on the copolymerization process, and the results compared with a linear model based filter design.

Introduction

Polymerization processes play an important role in chemical industries. The increasing demand for high quality polymers has motivated significant automation to provide the desired quality in the polymer products. However, as the level of automation increases, the process needs to be safeguarded against actuator and sensor faults. If not properly handled, they may cause issues such as off-spec product, plant shutdowns, economic losses or even safety hazards. Fault-handling, however, can only be achieved subsequent to Fault-detection and isolation (FDI). This realization has driven significant effort in the area of fault detection and isolation.

The most common approach to FDI is to employ information in the system model to diagnose faults. The approach is based on generating residuals, which are in some sense the difference between the expected and observed process behavior, by utilizing the analytical redundancy provided by the process model to generate state estimates. Additionally, thresholds are put in place to account for plant model mismatch and measurement noise, with an intent to avoid false alarms. There exists a plethora of results on FDI assuming linear process dynamics (see, e.g., [1], [2], [3] and [4]). However, these results may not remain effective for the copolymerization processes owing to the strong nonlinear characteristics of the process.

The FDI problem has also been considered for nonlinear systems subject to actuator faults, including approaches that utilize data-driven methods and those that generalize the problem to handle hybrid systems (see, e.g., [5], [6], [7], [8], [9] and [10]). In comparison to actuator faults, there exits fewer results on FDI for sensor faults (see, e.g., [4], [11], [12], [13] and [14]). The state estimation problem associated with FDI has been approached using different estimation techniques such as nonlinear observers [15], adaptive estimation

methods [16] or bank of high gain observers (see, e.g., [11] and [17]). Recently, a method that uses banks of high-gain observers was proposed to distinguish between actuator and sensor faults [18], where a system structure was assumed that enabled detection and isolation of all actuator and sensor faults. However, in some cases, as with the copolymerization process under consideration, the system structure does not allow the detection and isolation of all possible fault scenarios.

Motivated by the above considerations, in this work, we consider the copolymerization process and design an FDI mechanism cognizant of the fact that the system structure permits detection and isolation of only a subset of the faults. The rest of the manuscript is organized as follows: First, the polymerization process is described and a mathematical model for the process is presented. Next, we describe the control objectives for the polymerization reactor. Then, the nonlinear actuator and sensor fault isolation framework that recognizes the distinction between distinguishable and indistinguishable fault scenarios is designed. Also as a basis of comparison, linear FDI filters are designed by utilizing a linearized model for the process. The designed FDI filters are used to isolate faults for the polymerization process. Finally, we summarize our results in conclusion.

Process Description and Model

In this section, the MMA and VAc solution copolymerization process is described, where monomers A (MMA) and B (VAc) are continuously fed to a continuous-stirred tank reactor (CSTR) with initiator (azobisisobutyronitrile, AIBN), solvent (benzene), and chain transfer agent (acetaldehyde). A cooling jacket is equipped to remove the heat of the copolymerization reaction. The mathematical model for this reactor (in the absence of recycle streams and

inhibitors) is of the following form (see [10] and [19]):

$$\begin{aligned}
\dot{C}_j &= \left(\frac{Q_j}{M_j} - \frac{C_j \sum_k Q_k}{\rho}\right)\frac{1}{V} - R_j, \quad j = a, b, i, s, t \\
\dot{T}_R &= (T_0 - T_R)\frac{\sum_k Q_k}{\rho V} + [(-\Delta H_{paa})k_{paa}C_a C_{a\cdot} + (-\Delta H_{pba})k_{pba}C_a C_{b\cdot} \\
&\quad (-\Delta H_{pab})k_{pab}C_b C_{a\cdot} + (-\Delta H_{pbb})k_{pbb}C_b C_{b\cdot}]\frac{1}{\rho c_p} - \frac{UA(T_R - T_c)}{\rho c_p V}
\end{aligned} \tag{1}$$

where C_j is the concentration of species j, with subscript a, b, i, s, and t denoting monomer A, monomer B, initiator, solvent, and chain transfer agent, respectively, T_R is the temperature in the reactor, Q_k is the mass flow rate of species k, $k = a$, b, i, s, t, T_c is the temperature in the cooling jacket, M_j is the molar mass of species j, V is the volume of the reactor, ΔH is the enthalpy of the reaction, ρ and c_p are the density and the heat capacity of the fluid in the reactor, respectively, U is the overall heat transfer coefficient, A is the heat transfer area of the reactor, and

$$R_a = [(k_{paa} + k_{xaa})C_{a\cdot} + (k_{pba} + k_{xba})C_{b\cdot}]C_a$$

$$R_b = [(k_{pbb} + k_{xbb})C_{b\cdot} + (k_{pab} + k_{xab})C_{a\cdot}]C_b$$

$$R_i = k_i C_i$$

$$R_s = (k_{xas}C_{a\cdot} + k_{xbs}C_{b\cdot})C_s$$

$$R_t = (k_{xat}C_{a\cdot} + k_{xbt}C_{b\cdot})C_t$$

$$C_{a\cdot} = \frac{-l_2 + \sqrt{l_2^2 - 4l_1 l_3}}{2l_1}$$

$$C_{b\cdot} = \beta C_{a\cdot}$$

$$l_1 = k_{caa} + k_{daa} + 2\beta(k_{cab} + k_{dab}) + \beta^2(k_{cbb} + k_{dbb})$$

$$l_2 = 0$$

$$l_3 = -2k_i C_i \varepsilon$$

$$\beta = \frac{(k_{pab} + k_{xab})C_b}{(k_{pba} + k_{xba})C_a}$$

Each of the rate constants follows Arrhenius dependence on temperature described by:

$$k = A_k e^{-E/RT_R} \tag{3}$$

where A_k is the preexponential constant, E is the activation energy, and R is the ideal gas constant. The process parameters can be found in Table 1 (see also [10] and [19]).

The control objective under normal conditions is to operate the process at the nominal operating point, where $C_a = 2.5 \times 10^{-1}$ kmol/m^3, $C_b = 5.84$ kmol/m^3, $C_i = 2.0 \times 10^{-3}$ kmol/m^3, $C_s = 2.75$ kmol/m^3, $C_t = 3.7 \times 10^{-1}$ kmol/m^3, and $T_R = 350.5$ K. It is assumed that all the state measurements are available, and the flow rates Q_k, $k = a$, b, i, s, t, and T_c are chosen as manipulated input variables. The inputs are bounded as $0 \leq Q_a \leq 50$ kg/hr, $0 \leq Q_b \leq 120$ kg/hr, $0 \leq Q_i \leq 0.5$ kg/hr, $0 \leq Q_s \leq 100$ kg/hr, $0 \leq Q_t \leq 10$ kg/hr, and $320 \leq T_c \leq 350$ K. The steady state values of the inputs corresponding to the nominal operating point are $Q_a = 18$ kg/h, $Q_b = 90$ kg/h, $Q_i = 0.18$ kg/h, $Q_s = 36$ kg/h, $Q_t = 2.7$ kg/h, and $T_c = 336.15$ K.

The Lyapunov based nonlinear model predictive control design of [20] is implemented for the control purpose. The key feature of the MPC design is the implementation of a Lyapuonv function decay constraint to achieve stabilization (the formulation is reproduced in the Appendix). The hold-time for the control action is chosen as $\Delta = 6$ min, control horizon $T_c = 2\Delta$, and the prediction horizon $T_p = 10\Delta$. In the objective function, the states are normalized against ranges [0, 1], [0, 8], [0, 5×10^{-3}], [0, 10], [0, 1], and [340, 355], respectively, and the inputs are normalized using the magnitude of constraints. The matrices used to penalize the deviations of the normalized states from the steady state values and the increments of the inputs are chosen as Q_w and R_w, respectively. Q_w is a diagonal matrix with all diagonal arrays equal to 1 and R_w is a diagonal matrix with diagonal arrays equal

to 1, 1, 50, 0.5, 1, 1. The Lyapunov function is chosen to be a quadratic function of the form $V(x) = x'Px$, with

$$P = \begin{bmatrix} 22.9 & 3.60 & 3.99\times10^{3} & 0.01 & 5\times10^{-3} & 2.08 \\ 3.60 & 3.41 & 5.3\times10^{2} & 5\times10^{-3} & 5\times10^{-3} & 0.28 \\ 3.99\times10^{3} & 5.3\times10^{2} & 7.98\times10^{5} & 1.24 & 0.28 & 4.49\times10^{2} \\ 0.01 & 5\times10^{-3} & 1.24 & 2.98 & 2\times10^{-3} & 3\times10^{-4} \\ 5\times10^{-3} & 5\times10^{-3} & 0.28 & 2\times10^{-3} & 2.97 & 10^{-4} \\ 2.08 & 0.28 & 4.49\times10^{2} & 3\times10^{-4} & 10^{-4} & 0.52 \end{bmatrix}$$

Actuator and sensor fault isolation framework for the copolymerization process

In this section, we design a nonlinear actuator and sensor fault isolation framework for the copolymerization process. For comparison, we also design linear model based FDI filters by considering a linearized model of the process dynamics.

Nonlinear actuator and sensor fault isolation framework for the copolymerization process

The key idea is to exploit the analytical redundancy in the copolymerization process through state observer design using a bank of high-gain observers [17]. To this end, consider the description of the copolymerization process in the following form:

$$\begin{aligned} \dot{x} &= f(x) + G(x)(u + \tilde{u}) \\ y &= h(x) + \tilde{y} \end{aligned} \tag{4}$$

where $x \in \mathcal{X} \subset \mathbb{R}^n$ denotes the vector of state variables, with $\mathcal{X}$ being a compact set of the admissible state values, $u = [u_1, \ldots, u_m]^{\mathrm{T}} \in \mathbb{R}^m$ denotes the vector of prescribed control inputs, taking values in a nonempty compact convex set $\mathcal{U} \subseteq \mathbb{R}^m$, $\tilde{u} = [\tilde{u}_1, \ldots, \tilde{u}_m]^{\mathrm{T}} \in \mathbb{R}^m$ denotes the unknown fault vector for the actuators, $y = [y_1, \ldots, y_p]^{\mathrm{T}} \in \mathbb{R}^p$ denotes the vector

of output variables, $\tilde{y} = [\tilde{y}_1, \ldots, \tilde{y}_p]^{\mathrm{T}} \in \mathbb{R}^p$ denotes the unknown fault vector for the sensors, and $G(x) = [g_1(x), \ldots, g_m(x)]$. Due to the presence of physical constraints, the actual input $u + \tilde{u}$ implemented to the system takes values from the set $\mathcal{U}$ as well.

The design of the high gain observer requires the satisfaction of Assumption 1 below (and exploits the fact that the control action is computed using MPC and held constants over a sampling time):

Assumption 1. [21] There exist integers ω_i, $i = 1, \ldots, p$, with $\sum_{i=1}^{p} \omega_i = n$, and a coordinate transformation $\zeta = T(x, u)$ such that if $u = \bar{u}$, where $\bar{u} \in \mathcal{U}$ is a constant vector, then the representation of the system of Eq. (4) in the ζ coordinate takes the following form:

$$\begin{aligned} \dot{\zeta} &= A\zeta + B\phi(x, \bar{u}) \\ y &= C\zeta \end{aligned} \tag{5}$$

where $\zeta = [\zeta_1, \ldots, \zeta_p]^{\mathrm{T}} \in \mathbb{R}^n$, $A = \mathrm{blockdiag}[A_1, \ldots, A_p]$, $B = \mathrm{blockdiag}[B_1, \ldots, B_p]$, $C = \mathrm{blockdiag}[C_1, \ldots, C_p]$, $\phi = [\phi_1, \ldots, \phi_p]^{\mathrm{T}}$, $\zeta_i = [\zeta_{i,1}, \ldots, \zeta_{i,\omega_i}]^{\mathrm{T}}$, $A_i = \begin{bmatrix} 0 & I_{\omega_i - 1} \\ 0 & 0 \end{bmatrix}$, with $I_{\omega_i - 1}$ being a $(\omega_i - 1) \times (\omega_i - 1)$ identity matrix, $B_i = [0_{\omega_i - 1}^{\mathrm{T}}, 1]^{\mathrm{T}}$, with $0_{\omega_i - 1}$ being a vector of zeros of dimension $\omega_i - 1$, $C_i = [1, 0_{\omega_i - 1}^{\mathrm{T}}]$, and $\phi_i(x, \bar{u}) = \phi_{i,\omega_i}(x, \bar{u})$, with $\phi_{i,\omega_i}(x, \bar{u})$ defined through the successive differentiation of $h_i(x)$: $\phi_{i,1}(x, \bar{u}) = h_i(x)$ and $\phi_{i,j}(x, \bar{u}) = \frac{\partial \phi_{i,j-1}}{\partial x}[f(x) + g(x)\bar{u}], j = 2, \ldots, \omega_i$. Furthermore, $T : \mathbb{R}^n \times \mathcal{U} \to \mathbb{R}^n$ and $T^{-1} : \mathbb{R}^n \times \mathcal{U} \to \mathbb{R}^n$ are $\mathcal{C}^1$ functions on their domains of definition.

Assumption 1 describes the condition that the nonlinear system of Eq. 4 is observable from a given set of measured outputs. The bank of high gain observers is designed by leaving out subsets of the measured variables, subject to the satisfaction of Assumption 1 for the remaining measured variables (i.e., verifying whether the states can be estimated using the remaining measured variables). Assumption 1 does not hold when either C_s or C_t (or both)

are not measured. Note that since C_s and C_t do not appear on the right hand side of any state derivative expect $\dot{C}_s$ and $\dot{C}_t$, respectively, they are not observable unless directly measured. Thus transformation required in Assumption 1 does not hold for any subsets of sensors that do not include both C_s and C_t.

For a particular acceptable choice of a subset of sensors, $y = [C_a, C_b, C_i, C_s, C_t, T_R]$, for $t \in [t_k, t_{k+1})$, where $t_k = k\Delta$, $k = 0, \ldots, \infty$, the observer is formulated as follows:

$$\begin{aligned} \dot{\hat{\zeta}} &= A\hat{\zeta} + B\phi_0(\hat{x}, u(t_k)) + H(y - C\hat{\zeta}) \\ \hat{\zeta}(t_k) &= T(\hat{x}(t_k), u(t_k)) \end{aligned} \tag{6}$$

where $\hat{x}$ and $\hat{\zeta}$ denote the estimates of x and ζ, respectively, $H = \text{blockdiag}[H_1, \ldots, H_p]$ is the observer gain, $H_i = \left[\frac{a_{i,1}}{\varepsilon}, \ldots, \frac{a_{i,\omega_i}}{\varepsilon^{\omega_i}}\right]^{\mathrm{T}}$, with $s^{\omega_i} + a_{i,1}s^{\omega_i - 1} + \cdots + a_{i,\omega_i} = 0$ being a Hurwitz polynomial and ε being a positive constant to be specified, $\hat{x}(t_k) = T^{-1}(\hat{\zeta}(t_k^-), u(t_{k-1}))$ for $k = 1, \ldots, \infty$, and ϕ_0 is the nominal model of ϕ. The state observer requires the global boundedness of ϕ_0 as it is presented in Assumption 2.

Assumption 2. [18] $\phi_0(x, u)$ is a $\mathcal{C}^0$ function on its domain of definition and globally bounded in x.

In this work, we consider each fault scenario comprising at most two simultaneous faults. Thus with m actuators and p sensors, the total number of possible fault scenarios n_f is

$$n_f = C_1^m C_0^p + C_0^m C_1^p + C_1^m C_1^p + C_2^m C_0^p + C_0^m C_2^p = m + p + mp + \frac{m(m-1)}{2} + \frac{p(p-1)}{2} \tag{7}$$

where C_k^n presents the binomial coefficients which is equal to $\binom{n}{k} = \frac{n}{k!(n-k)!}$. For the copolymerization process, given that there are six actuators and six sensors, and considering at most two simultaneous faults, there exist a total $2 \times C_0^6 C_1^6 + C_1^6 C_1^6 + 2 \times C_0^6 C_2^6 = 78$ possible scenarios.

For each fault scenario, the objective is to define a residual as the norm of the difference between the state prediction and the state estimate for the subsystem (appropriately defined) corresponding to the fault scenario. The expected process trajectory is computed using the subsystem of the process model that is independent of the specific actuator fault (if that is included in that particular fault scenario) and the state estimates generated by the observer that does not utilize the particular sensor (if that is included in that particular fault scenario), and is not directly effected by the particular actuator. This expected trajectory when compared with the observed trajectory to generate residuals results in each residual being sensitive to a unique subset of faults.

The system structure perquisite for generating such state estimates is presented in Assumption 3. To this end, let $\theta_{f,i}$ denote the fault vector (sensor/and or actuator) for the ith fault scenario, and $\bar{\theta}_{f,i}$ the remaining fault variable vector (the remaining $\tilde{u}$ and $\tilde{y}$ variables). Specifically, let $u_{f,i}$ and $y_{f,i}$ denote the vectors of input and output variables subject to faults $\theta_{f,i}$, respectively. Let $\bar{u}_{f,i}$ and $\bar{y}_{f,i}$ denote the vectors of the rest of the input and output variables, respectively.

Assumption 3. [18] Assumptions 1 and 2 hold for the system of Eq. (4), with $\bar{u}_{f,i}$ and $\bar{y}_{f,i}$ being the vectors of input and output variables, respectively, $i = 1, \ldots, n_f$.

Under Assumption 3, the state observer for the ith fault scenario is designed as follow :

$$\begin{aligned} \dot{\hat{\zeta}}^j &= A^j \hat{\zeta}^j + H^j(\bar{y}_{f,i} - C^j \hat{\zeta}^j) \\ \dot{\hat{\zeta}}^j(t_k) &= T^j(\hat{x}^j(t_k), \bar{u}_{f,i}(t_k)) \end{aligned} \tag{8}$$

where j presents the jth observer.

We now describe how residuals are generated for the copolymerization process for the fault vectors for which Assumption 3 is satisfied. For example, consider a single actuator

fault in $\theta_{f,11} = \tilde{u}_6$ (corresponding to faults in the actuator for T_c), the corresponding state prediction is computed by first considering the subsystem for which $u_6 = T_c$ does not appear on the right-hand side of the corresponding ordinary differential equations (ODE's):

$$\begin{aligned}
\dot{C}_a &= \left(\frac{Q_a}{M_a} - \frac{C_a \sum_k Q_k}{\rho}\right)\frac{1}{V} - R_a(C_a, C_b, C_i, T_R) \\
\dot{C}_b &= \left(\frac{Q_b}{M_b} - \frac{C_b \sum_k Q_k}{\rho}\right)\frac{1}{V} - R_b(C_a, C_b, C_i, T_R) \\
\dot{C}_i &= \left(\frac{Q_i}{M_i} - \frac{C_i \sum_k Q_k}{\rho}\right)\frac{1}{V} - R_i(C_i, T_R) \\
\dot{C}_s &= \left(\frac{Q_s}{M_s} - \frac{C_s \sum_k Q_k}{\rho}\right)\frac{1}{V} - R_s(C_a, C_b, C_i, T_R) \\
\dot{C}_t &= \left(\frac{Q_t}{M_t} - \frac{C_t \sum_k Q_k}{\rho}\right)\frac{1}{V} - R_t(C_a, C_b, C_i, T_R)
\end{aligned} \tag{9}$$

In particular, the prediction model does not include T_R as one of its states and wherever T_R appears on the right hand side of corresponding ODE's (which affects the dynamics of the other prediction states), its estimated value, $\bar{T}_R$ is used. Therefore, the model used to generate predictions for this filter takes the following form:

$$\begin{aligned}
\dot{\tilde{C}}_a &= \left(\frac{Q_a}{M_a} - \frac{\tilde{C}_a \sum_k Q_k}{\rho}\right)\frac{1}{V} - R_a(\tilde{C}_a, \tilde{C}_b, \tilde{C}_i, \bar{T}_R) \\
\dot{\tilde{C}}_b &= \left(\frac{Q_b}{M_b} - \frac{\tilde{C}_b \sum_k Q_k}{\rho}\right)\frac{1}{V} - R_b(\tilde{C}_a, \tilde{C}_b, \tilde{C}_i, \bar{T}_R) \\
\dot{\tilde{C}}_i &= \left(\frac{Q_i}{M_i} - \frac{\tilde{C}_i \sum_k Q_k}{\rho}\right)\frac{1}{V} - R_i(\tilde{C}_i, \bar{T}_R) \\
\dot{\tilde{C}}_s &= \left(\frac{Q_s}{M_s} - \frac{\tilde{C}_s \sum_k Q_k}{\rho}\right)\frac{1}{V} - R_s(\tilde{C}_a, \tilde{C}_b, \tilde{C}_i, \bar{T}_R) \\
\dot{\tilde{C}}_t &= \left(\frac{Q_t}{M_t} - \frac{\tilde{C}_t \sum_k Q_k}{\rho}\right)\frac{1}{V} - R_t(\tilde{C}_a, \tilde{C}_b, \tilde{C}_i, \bar{T}_R)
\end{aligned} \tag{10}$$

where $\tilde{(\cdot)}$ denotes the predicted value for a particular variable and $\bar{(\cdot)}$ denotes the corresponding estimate.

In Eq. 10, the predicted values ($\tilde{C}_j$, where $j = a, b, i, s, t$) are the expected trajectories of

states computed using the prediction model presented as Eq. 10. The estimate $\bar{T}_R$ for use in the above prediction is generated by designing a high gain observer that uses measurements of $y_1 = C_{\rm a}$, $y_2 = C_{\rm b}$, $y_3 = C_{\rm i}$, $y_4 = C_{\rm s}$ and $y_5 = C_t$. The coordinate transformation for this observer is as follows: $\zeta^1_{1,1} = C_{\rm a}$, $\zeta^1_{2,1} = C_{\rm b}$, $\zeta^1_{2,2} = \dot{C}_{\rm b}$, $\zeta^1_{3,1} = C_{\rm i}$, $\zeta^1_{4,1} = C_{\rm s}$, and $\zeta^1_{5,1} = C_{\rm t}$, and uses the fact that the input action is computed in a discrete fashion (see [17] for further details). The observer design is as follows:

$$\begin{aligned}
\dot{\hat{\zeta}}_{1,1} &= \frac{a_{1,1}}{\varepsilon}(y_1 - \hat{\zeta}_{1,1}) \\
\dot{\hat{\zeta}}_{2,1} &= \hat{\zeta}_{2,2} + \frac{a_{2,1}}{\varepsilon}(y_2 - \hat{\zeta}_{2,1}) \\
\dot{\hat{\zeta}}_{2,2} &= \frac{a_{2,2}}{\varepsilon^2}(y_2 - \hat{\zeta}_{2,1}) \\
\dot{\hat{\zeta}}_{3,1} &= \frac{a_{3,1}}{\varepsilon}(y_3 - \hat{\zeta}_{3,1}) \\
\dot{\hat{\zeta}}_{4,1} &= \frac{a_{4,1}}{\varepsilon}(y_4 - \hat{\zeta}_{4,1}) \\
\dot{\hat{\zeta}}_{5,1} &= \frac{a_{5,1}}{\varepsilon}(y_5 - \hat{\zeta}_{5,1})
\end{aligned} \tag{11}$$

with $\varepsilon = 0.04$, $a_{i,1} = 5$, and $a_{i,2} = 100$, i =1, 2, 3, 4. The other observers required for the implementation of the rest of the filters are also designed in a similar fashion with the same values of the observer parameters. Among these observers, four are designed using five outputs corresponding to single or multiple fault scenarios (single sensor or single actuators faults or simultaneous sensor and actuator faults), and six using four outputs, corresponding to multiple fault scenarios (two sensors or simultaneous sensor and actuator faults).

The dedicated residual for a fault in $u_6 = T_c$ (with $\theta_{f,i} = \tilde{T}_c$) is then defined as

$$r_{11} = \sqrt{(\tilde{C}_{\rm a} - \bar{C}_{\rm a})^2 + (\tilde{C}_{\rm b} - \bar{C}_{\rm b})^2 + (\tilde{C}_{\rm i} - \bar{C}_{\rm i})^2 + (\tilde{C}_{\rm s} - \bar{C}_{\rm s})^2 + (\tilde{C}_{\rm t} - \bar{C}_{\rm t})^2}$$

When a fault takes place in T_c only, the estimates of the states (utilized in the present filter) stay accurate, because the value of T_c is not utilized to generate the estimates. Furthermore, the subsystem has been chosen to be independent of T_c, therefore the predicted

values stay the same as the true values, which are in turn being correctly estimated. Thus, this residual stays close to zero.

On the other hand, consider $\theta_{f,1} = \tilde{C}_a$ for which a residual r_1 needs to be designed. The model used to generate predictions for this filter takes the form:

$$
\begin{aligned}
\dot{\tilde{C}}_a &= \left(\frac{Q_a}{M_a} - \frac{\tilde{C}_a \sum_k Q_k}{\rho}\right)\frac{1}{V} - R_a(\tilde{C}_a, \tilde{C}_b, \tilde{C}_i, \tilde{T}_R) \\
\dot{\tilde{C}}_b &= \left(\frac{Q_b}{M_b} - \frac{\tilde{C}_b \sum_k Q_k}{\rho}\right)\frac{1}{V} - R_b(\tilde{C}_a, \tilde{C}_b, \tilde{C}_i, \tilde{T}_R) \\
\dot{\tilde{C}}_i &= \left(\frac{Q_i}{M_i} - \frac{\tilde{C}_i \sum_k Q_k}{\rho}\right)\frac{1}{V} - R_i(\tilde{C}_i, \tilde{T}_R) \\
\dot{\tilde{C}}_s &= \left(\frac{Q_s}{M_s} - \frac{\tilde{C}_s \sum_k Q_k}{\rho}\right)\frac{1}{V} - R_s(\tilde{C}_a, \tilde{C}_b, \tilde{C}_i, \tilde{T}_R) \\
\dot{\tilde{C}}_t &= \left(\frac{Q_t}{M_t} - \frac{\tilde{C}_t \sum_k Q_k}{\rho}\right)\frac{1}{V} - R_t(\tilde{C}_a, \tilde{C}_b, \tilde{C}_i, \tilde{T}_R) \\
\dot{\tilde{T}}_R &= (T_0 - \tilde{T}_R)\frac{\sum_k Q_k}{\rho V} + [(-\Delta H_{paa})k_{paa}\tilde{C}_a C_{a\cdot} + (-\Delta H_{pba})k_{pba}\tilde{C}_a C_{b\cdot} \\
&\quad (-\Delta H_{pab})k_{pab}\tilde{C}_b C_{a\cdot} + (-\Delta H_{pbb})k_{pbb}\tilde{C}_b C_{b\cdot}]\frac{1}{\rho c_p} - \frac{UA(\tilde{T}_R - T_c)}{\rho c_p V}
\end{aligned}
\tag{12}
$$

To estimate $\bar{C}_a$, a high gain observer is designed that uses measurements of $y_2 = C_{\mathrm{b}}$, $y_3 = C_{\mathrm{i}}$, $y_4 = C_{\mathrm{s}}$, $y_5 = C_t$, $y_6 = T_R$. The coordinate transformation for this observer is as follows: $\zeta^1_{1,1} = C_{\mathrm{b}}$, $\zeta^1_{1,2} = \dot{C}_{\mathrm{b}}$, $\zeta^1_{2,1} = C_{\mathrm{i}}$, $\zeta^1_{3,1} = C_{\mathrm{s}}$, $\zeta^1_{4,1} = C_{\mathrm{t}}$, and $\zeta^1_{5,1} = T_{\mathrm{R}}$. The observer

design is as follows:

$$\begin{aligned}
\dot{\hat{\zeta}}_{1,1} &= \hat{\zeta}_{1,2} + \frac{a_{1,1}}{\varepsilon}(y_2 - \hat{\zeta}_{1,1}) \\
\dot{\hat{\zeta}}_{1,2} &= \frac{a_{1,2}}{\varepsilon^2}(y_2 - \hat{\zeta}_{1,1}) \\
\dot{\hat{\zeta}}_{2,1} &= \frac{a_{2,1}}{\varepsilon}(y_3 - \hat{\zeta}_{2,1}) \\
\dot{\hat{\zeta}}_{3,1} &= \frac{a_{3,1}}{\varepsilon}(y_4 - \hat{\zeta}_{3,1}) \\
\dot{\hat{\zeta}}_{4,1} &= \frac{a_{4,1}}{\varepsilon}(y_5 - \hat{\zeta}_{4,1}) \\
\dot{\hat{\zeta}}_{5,1} &= \frac{a_{5,1}}{\varepsilon}(y_6 - \hat{\zeta}_{5,1})
\end{aligned} \tag{13}$$

The residual for r_1 is defined as follows:

$$r_1 = \sqrt{(\tilde{C}_\mathrm{a} - \bar{C}_\mathrm{a})^2 + (\tilde{C}_\mathrm{b} - \bar{C}_\mathrm{b})^2 + (\tilde{C}_\mathrm{i} - \bar{C}_\mathrm{i})^2 + (\tilde{C}_\mathrm{s} - \bar{C}_\mathrm{s})^2 + (\tilde{C}_\mathrm{t} - \bar{C}_\mathrm{t})^2 + (\tilde{T}_\mathrm{R} - \bar{T}_\mathrm{R})^2}$$

Note that the evolution of T_R is directly affected by the fault in T_c, and the estimated value of T_R being accurate, it will therefore also be affected by the fault in T_c. However, the prediction model uses the expected or computed value of T_c, therefore the evolution of the states in the prediction model ends up being different from the true evolution. Thus, r_1 breaches its threshold. The rest of the residuals are designed in a similar fashion, and every filter that uses the computed values of T_c ends up breaching the threshold. In particular, all the residuals breach their thresholds except for r_{11} (the dedicated filter for T_c), r_{12}, r_{13}, r_{14} and r_{15} (filters dedicated for T_c, and a sensor fault). By looking at these residuals, one can deduce that either a fault in T_c, or a fault in T_c and one of the sensors must have taken place. However, since breaching all the dedicated residuals for the sensor faults indicate no fault in any of the sensors, by the process of elimination it can be concluded that a single actuator fault in T_c must have taken place. The rest of the fault isolation logic is determined in a similar fashion.

Remark 1. Note that the system structure does not satisfy the standard assumptions for

high gain observer design (e.g., [22], [23]). However, the recognition that the control action is implemented in a discrete fashion allows invoking the relaxation on the system structure, as presented in [17]. This in turn enables the design of the high-gain observers required for the purpose of building the bank of observers that constitute the FDI filters.

Now consider $\theta_{f,i} = \tilde{y}_4 = \tilde{C}_s$. Since $\theta_{f,i} = \tilde{C}_s$ does not include any input fault, the corresponding prediction model takes the same form as it is described in Eq. 12. To estimate $\bar{C}_s$, a high gain observer needs to be designed that uses measurements of $y_2 = C_{\mathrm{b}}$, $y_3 = C_{\mathrm{i}}$, $y_4 = C_{\mathrm{s}}$, $y_5 = C_t$, $y_6 = T_R$. To design the corresponding observer, the required transformation in Assumption 1 must exist. However, since C_s is fundamentally unobservable, the required transformation in Assumption 1 does not exist and the corresponding high gain observer which is insensitive to fault in $y_4 = C_s$ can not be designed. Thus, the corresponding insensitive residual to $\theta_{f,i} = \tilde{C}_s$ is undefined and when fault in $y_4 = C_s$ takes place, all of the existing residuals breach their thresholds, and also all the residuals breach thresholds when say a fault in $y_5 = C_t$ takes place making it impossible to isolate whether a fault has taken place in $y_4 = C_s$ or $y_5 = C_t$. Lets consider another example, when $\theta_{f,i} = \tilde{u}_1 = \tilde{Q}_a$. To define the corresponding prediction model, the subsystem which is not subject to fault input must be used. However, since $u_1 = Q_a$ appears in all of the state equations (see Eq. 1), therefore the corresponding prediction model does not exist and as a result the corresponding insensitive residual to $\theta_{f,i} = \tilde{Q}_a$ is undefined. Thus when fault in $u_1 = Q_1$ takes places, all of the existing residuals breach their thresholds and fault in $u_1 = Q_1$ can not be isolated.

Motivated by above considerations, we first define distinguishable faults scenarios as those for which if that particular fault-scenario occurs, there exists an FDI mechanism that can be used to determine uniquely (based on the evolution of the measurements), the occurrence of

that fault scenario. Corollary 1 presents the necessary and sufficient conditions for a fault scenario to be distinguishable. The proof is omitted here since it follows the same line of arguments as the proof of Proposition 1 and Theorem 1 in [18]. To this end, let $r_{i,ins}$ denote the vector of corresponding insensitive residuals to the *ith* fault scenario, as defined in [18].

Corollary 1. *Consider the system of Eq. 4, for which Assumptions 1-3 hold. A fault scenario $\theta_{f,i}$, where $\theta_{f,i} = \tilde{y}_f$ or $\theta_{f,i} = \tilde{u}_f$ is distinguishable if and only if there exists a one-to-one mapping between every fault scenario and $r_{i,ins}$, where $i \in \{1, \ldots, n_f\}$. Furthermore, any $\theta_{f,i}$ that comprises combinations of distinguishable fault scenarios is distinguishable and combination of an indistinguishable fault scenario with any fault scenario is indistinguishable.*

Corollary 1 classifies faults in two categories; distinguishable ($\theta_{f,dis}$) and indistinguishable ($\theta_{f,indis}$) faults. Each fault scenario belongs only to one of these categories. If m_{dis} of the inputs and p_{dis} of the outputs (when considered in isolation) satisfy the conditions in Corollary 1, the cardinality of set $\theta_{f,dis}$ is

$$\begin{aligned} C_1^{m_{dis}} C_0^{p_{dis}} + C_0^{m_{dis}} C_1^{p_{dis}} + C_1^{m_{dis}} C_1^{p_{dis}} + C_2^{m_{dis}} C_0^{p_{dis}} + C_0^{m_{dis}} C_2^{p_{dis}} = \\ m_{dis} + p_{dis} + m_{dis} p_{dis} + \frac{m_{dis}(m_{dis}-1)}{2} + \frac{p_{dis}(p_{dis}-1)}{2} \end{aligned} \tag{14}$$

Furthermore, since $\theta_{f,dis}$ and $\theta_{f,indis}$ are complement of each other, therefore the cardinality of set $\theta_{f,indis}$ is $n_f - |\theta_{f,dis}|$.

For the copolymerization process $y_4 = C_s$ and $y_5 = C_t$ are fundamentally unobservable, and $u_1 = Q_a$ or $u_2 = Q_b$ or $u_3 = Q_i$ or $u_4 = Q_s$ or $u_5 = Q_t$ appears in all of the state equations resulting in prediction model to be undefined for them. Thus for single fault in any of these actuators or sensors, the corresponding insensitive residuals are undefined. Thus $m_{dis} = 1$, and $p_{dis} = 4$, therefore only $C_0^1 C_1^4 + C_1^1 C_0^4 + C_1^1 C_1^4 + C_2^4 = 15$ scenarios are distinguishable. The rest of the 63 fault scenarios belong to $\theta_{f,indis}$.

With the recognition that some of fault scenarios are indistinguishable, the FDI scheme is still able to detect the indistinguishable faults and confine the possible scenarios for fault location to all possible combinations of indistinguishable actuators and sensors. Theorem 1 presents the mechanism for detecting and limiting the possible locations for indistinguishable actuators and sensors. To this end, consider the system of Eq. (4), where at most two simultaneous faults can occur and let δ_i denote the threshold for the ith fault scenario and $t_{k'}$ be the time by which all of the residuals have breached their threshold i.e., $r_{i,k} > \delta_i$ $\forall i \in \{1, \ldots, |\theta_{f,dis}|\}$.

Theorem 1. *Consider the system of Eq. (4), for which Assumption 1-3 hold. If* $t_k \geq t_{k'}$ *then* $\theta_{f,indis}(t) \neq 0$ *for some* $t \in [t_{k'}, t_k)$.

Proof. First, note that $r_{i,k} > \delta_i$ $\forall i \in \{1, \ldots, |\theta_{f,dis}|\}$, we know that some $\theta_{f_i} > 0$. We then show that some fault scenario $\theta_{f,indis}$ take place by contradiction argument. To this end, lets assume that $\theta_{f,dis}$ take place. Therefore $r_{i,k} \leq \delta_i$ for at least one $i \in \{1, \ldots, |\theta_{f,dis}|\}$ (Theorem 1 in [18]). However, this is in contradiction with $r_{i,k} > \delta_i$ for all $i \in \{1, \ldots, |\theta_{f,dis}|\}$. Thus $\theta_{f,indis}(t) \neq 0$ for some $t \in [t_{k'}, t_k)$. This concludes the proof of Theorem 1. □

As a result of Theorem 1, the design acts as a fault detection mechanism for faults in $y_4 = C_s$, $y_5 = C_t$, $u_1 = Q_a$, $u_2 = Q_b$, $u_3 = Q_i$, $u_4 = Q_s$, $u_5 = Q_t$ or any combination of them. In particular, if a fault takes place in any of these, all of the residuals are expected to breach their thresholds, resulting in fault detection. However, isolation of the fault is not achieved. Note that this is a fundamental limitation of the process, and not of the FDI framework. The FDI framework, however, clearly points to this realization, which can be utilized at the design stage to wisely invest in 'smart' or redundant sensors and actuators for these variables to achieve FDI.

Linear FDI filters for the copolymerization process

In this section, we design linear FDI filters for the copolymerization process to compare results obtained from the FDI nonlinear filters with model based linear FDI filters. However, because of lack of result in the literature on simultaneous actuator and sensor fault isolation design for linear systems (see e.g., [1], [24], [25] and [26]), the FDI linear filters are also designed based on [18] by considering a linearized model for the copolymerization process. The only difference here is the residuals are defined as the norm of difference between the state prediction and the output measurements for the subsystem corresponding to the fault scenario. A fault is detected and isolated when the corresponding residuals breach their thresholds. For example when a fault takes place in y_1, only r_1, r_5, r_6, r_7, r_{13} breach their thresholds. By investigating these residuals, it can be deduced that either a fault in $y_1 = C_{\mathrm{a}}$ or a fault in $y_1 = C_{\mathrm{a}}$ and one of other sensors or a fault in $y_1 = C_{\mathrm{a}}$ and the single actuator must have taken place. However, since the dedicated residual for other single sensor faults and the single actuator fault do not breach their residuals, by using a process of elimination it can be concluded that a single sensor fault in C_{a} must have taken place. As with the nonlinear FDI filters, because of existence of unobservable outputs (C_s and C_t) and appearance of five of the six inputs (Q_a, Q_b, Q_i, Q_s and Q_t) in all of the model equations, we can only design 15 residuals.

Remark 2. Note that the presence of the FDI mechanism enables FDI in the closed-loop system thereby allowing the operator to determine the appropriate course of action following a fault. For instance, in the case of a single actuator fault, if the fault is simply a constant bias fault, then a robust/offset free controller would still keep the process operating at the desired operating point. Knowing through the FDI mechanism that a sensor fault has not taken

place can help the operator prioritize the correction of such an actuator at a later stage. On the other hand, with the FDI determining a single actuator fault, if the functioning sensors reveal that the process is moving off-spec, or the control action starts chattering (perhaps because the existing robust/offset free controller is not able to handle the particular kind of actuator fault), the operator can then trigger reconfiguration (e.g., [6]) and actuator repair on a more urgent basis. For sensor faults, on the other hand, even if its a constant bias fault, there exists no control law that can drive the process to the desired set-point for the variable in question. The FDI information then becomes critical in taking that sensor out of the loop (where possible), or triggering immediate recertification of the sensor to preserve on-spec production.

Remark 3. Note that there exist so called smart sensors and actuators that could potentially also be used for purpose of fault diagnosis. These are inherently based on the principle of physical redundancy. For instance, a smart actuator for a valve would have an additional means of 'measuring' the valve opening which can then be compared to the prescribed value to detect and isolate the fault. The proposed FDI approach is not intended to replace the smart sensors and actuators, but instead to complement these, and also point to where such devices are required for the purpose of FDI. In particular, the proposed FDI approach can be utilized, where possible, to achieve FDI for number of sensors and actuators to mitigate the high installation and maintenance cost of smart sensors. For more safety critical sensors and actuators, the model based approach can be utilized to provide an additional layer of redundancy to the smart devices. Finally, a rigorous FDI design points, as with the copolymerization process, to the requirement of smart devices for certain subsets of sensors and actuators where fault isolation is not possible otherwise.

Remark 4. Note that in the present manuscript, the high gain observers are only used for the purpose of illustration. Any other estimation scheme such as moving horizon estimation (MHE) could also be used. The critical requirement being the ability for the estimates to converge at a sufficiently fast rate. Note that successful FDI relies on accurate enough state estimation, in the absence of which the FDI filters will lead to either missed detection or false alarms.

Application of the actuator and sensor fault isolation framework

In this section, we apply the proposed FDI filters to the process. Practical issues such as parametric uncertainty, time-varying disturbances, and measurement noise are considered in the simulations. Specifically, the values of A_{pbb}, A_{xas}, A_{xbs}, A_{xat}, and A_{xbt} are 10% smaller than their nominal value and A_{xbb} is 10% larger. The bounds on these uncertainty are $\pm 10\%$ of their nominal values. The inlet streams of monomer B and solvent contain small amounts of the other. The mass fraction of monomer B in the flow of solvent varies according to $0.02 + 0.02\sin(t)$, and the mass fraction of solvent in the flow of monomer B varies as $0.01 + 0.01\sin(2t)$. The concentration and temperature measurements have combinations of 5 Hz sinusoidal noises. The measurement noise has a normal distribution of variance 0.02, 0.2, 0.0005, 0.2, 0.02, and 0.5 in C_a, C_b, C_i, C_s, C_t, and T_R, respectively. It is assumed that measurements are sampled 10 times evenly between two successive times when control action is implemented. The noisy measurement are processed through a first order low pass filter with time constant equal to 3 min.

To account for the presence of disturbances and measurement noise, thresholds for each

filter were determined based on normal operation, and are reported in Tables 2 and 3. In particular, the maximum observed value of each residual when operating at steady state is selected as the corresponding threshold. It should be noted that thresholds values for the linear filters are relatively higher than the nonlinear filters. This is because the estimation error when using the linear model based state observer converges to larger values even in the absence of faults.

To ascertain that both filter designs work, we first consider a case where a large abrupt, constant bias fault of magnitude 0.5 $kmol/m^3$ in $y_1 = C_a$ (single sensor fault) takes place at time $t_f = 1.5$ hr. The evolution of residual profiles is shown in Fig. 1, where the FDI logic is able to achieve FDI using both filter designs.

We next consider a fault of smaller magnitude (0.05 $kmol/m^3$). In particular, we consider a case where an abrupt, constant bias fault in $y_1 = C_a$ (single sensor fault) takes place at time $t_f = 1.5$ hr. The evolution of the measurements of the output variables, the state estimates provided by the observer that uses measurements of C_{b}, C_{i}, C_{s}, C_{t} and T_{R}, and the true values of the state variables are depicted by solid, dashed, and dashed-dotted lines in Fig. 2, respectively. The evolution of residual profiles is shown in Fig. 1. It can be seen that some of the filters breach their threshold for the linear FDI design. In essence, the fault is successfully detected but is not isolated since the residual profiles does not follow any of the expected patterns. In contrast, the nonlinear FDI design successfully detects and isolates the fault.

We next consider a case where incipient faults in $y_1 = C_{\rm a}$ and $u_6 = T_{\rm c}$ (one actuator fault and one sensor fault) take place, starting at time $t_f = 1.5$ hr. The faults are simulated as follows:

$$\tilde{y}_1 = \begin{cases} 0, & 0 \le t < t_f \\ (0.05 + 0.05\sin 5t)(2 - e^{5t_f - 5t}), & t \ge t_f \end{cases}$$
$$\tilde{u}_6 = \begin{cases} 0, & 0 \le t < t_f \\ (5 + 5\sin 5t)(2 - e^{5t_f - 5t}), & t \ge t_f \end{cases} \tag{15}$$

The evolution of residual profiles is shown in Fig. 3. Like the previous case, using the linear FDI method, some of the residuals breach their thresholds and therefore the fault is successfully detected. However, the fault is not isolated since residual profiles does not follow any of expected patterns. In contrast, by using the proposed method, the fault in y_1 and u_6 is successfully isolated.

The FDI results for other distinguishable faults scenarios were also considered and are not presented here for sake of brevity. Finally, we demonstrate the ability to detect the indistinguishable faults. In particular, we consider a case where faults take place in $y_4 = C_s$ and $u_1 = Q_a$ at time $t_f = 1.5$hr, simulated as follows:

$$\tilde{y}_4 = \begin{cases} 0, & 0 \le t < t_f \\ (0.55 + 0.55\sin 5t)(2 - e^{5t_f - 5t}), & t \ge t_f \end{cases}$$
$$\tilde{u}_1 = \begin{cases} 0, & 0 \le t < t_f \\ (3.5 + 3.5\sin 5t)(2 - e^{5t_f - 5t}), & t \ge t_f \end{cases} \tag{16}$$

The evolution of residual profiles is shown in Fig. 4. As it is mentioned in Theorem 1, since all the residuals breach their thresholds, the fault is successfully detected. However, the fault can not be in any of considered scenarios in FDI filters design, since all of the residual

have breached their thresholds. Therefore according to the Theorem 1, the fault must be in either $y_4 = C_s$ or $y_5 = C_t$ or $u_1 = Q_a$, $u_2 = Q_b$, $u_3 = Q_i$, $u_4 = Q_s$, $u_5 = Q_t$ or any combination of these actuator and sensor faults.

Remark 5. In essence, the linear FDI method is only able to detect, but not isolate faults in the copolymerization process. This is primarily due to the estimation and prediction errors associated with using a linear model in the observer, prediction model and filter design. The high gain observer can readily be replaced by other observers (such as the Kalman filter, extended Kalman filter, or the moving horizon observers), which can improve the estimation accuracy of the observer; however, the errors associated with prediction using a linear model will still remain limiting the effectiveness of linear model based FDI designs.

Remark 6. From fault handling perspective, sensor faults can be handled by using estimation of states that are verified to be accurate, instead of using a faulty sensor reading (as is done in the simulation results corresponding to Figure 2). The actuator faults on the other hand directly impact the control action implemented on the plant, and if not handled, could result in the states deviating from nominal operating point. In this case, once such a fault has been detected, robust control methods or control reconfiguration methods can be used to achieve fault-tolerant control (see, e.g., [6]). To handle actuator and sensor faults simultaneously, both sensor and actuator handling approaches would have to be implemented simultaneously.

Conclusions

This work considered the problem of isolating actuator and sensor faults in the solution copolymerization of MMA and VAc. To achieve fault detection and isolation for the copolymerization reactor, an actuator and sensor fault isolation framework was designed. The key

idea is to exploit the analytical redundancy in the copolymerization model through state observer design using bank of high gain observers. The ability of the proposed framework in detecting and determining possible locations for indistinguishable fault scenarios was proved and verified through simulations. Illustrative linear FDI filters were also designed for the purpose of comparison. While linear model based FDI only achieved fault detection, the application of the proposed FDI mechanism was found to also successfully isolate distinguishable faults even in the presence of plant-model mismatch and measurement noise.

Acknowledgments

Financial support from the McMaster Advanced Control Consortium is gratefully acknowledged.

Literature Cited

[1] Frank PM. Fault diagnosis in dynamic systems using analytical and knowledge-based redundancy: A survey and some new results. *Automatica*. 1990;26(3):459–474.

[2] Edwards C, Spurgeon SK, Patton RJ. Sliding mode observers for fault detection and isolation. *Automatica*. 2000;36(4):541–553.

[3] Venkatasubramanian V, Rengaswamy R, Yin K, Kavuri SN. A review of process fault detection and diagnosis: Part I: Quantitative model-based methods. *Computers & chemical engineering*. 2003;27(3):293–311.

[4] Tong C, El-Farra NH, Palazoglu A, Yan X. Fault detection and isolation in hybrid process systems using a combined data-driven and observer-design methodology. *AIChE Journal*. 2014;60(8):2805–2814.

[5] De Persis C, Isidori A. A geometric approach to nonlinear fault detection and isolation. *Automatic Control, IEEE Transactions on*. 2001;46(6):853–865.

[6] Mhaskar P, McFall C, Gani A, Christofides PD, Davis JF. Isolation and handling of actuator faults in nonlinear systems. *Automatica*. 2008;44(1):53–62.

[7] Zhang X, Polycarpou MM, Parisini T. Fault diagnosis of a class of nonlinear uncertain systems with Lipschitz nonlinearities using adaptive estimation. *Automatica*. 2010; 46(2):290–299.

[8] Chilin D, Liu J, Muñoz de la Peña D, Christofides PD, Davis JF. Detection, isolation and handling of actuator faults in distributed model predictive control systems. *Journal of Process Control*. 2010;20(9):1059–1075.

[9] Hu Y, El-Farra NH. Robust fault detection and monitoring of hybrid process systems with uncertain mode transitions. *AIChE Journal*. 2011;57(10):2783–2794.

[10] Du M, Mhaskar P. Active fault isolation of nonlinear process systems. *AIChE Journal*. 2013;59(7):2435–2453.

[11] Mattei M, Paviglianiti G, Scordamaglia V. Nonlinear observers with H_∞ performance for sensor fault detection and isolation: a linear matrix inequality design procedure. *Contr Eng Prac*. 2005;13:1271–1281.

[12] Perk S, Teymour F, Cinar A. Adaptive agent-based system for process fault diagnosis. *Industrial & Engineering Chemistry Research*. 2011;50(15):9138–9155.

[13] MacGregor J, Cinar A. Monitoring, fault diagnosis, fault-tolerant control and optimization: Data driven methods. *Computers & Chemical Engineering*. 2012;47:111–120.

[14] Mhaskar P, Liu J, Christofides P. *Fault-tolerant process control*. Springer. 2013.

[15] Rajamani R, Ganguli A. Sensor fault diagnostics for a class of non-linear systems using linear matrix inequalities. *International Journal of Control*. 2004;77(10):920–930.

[16] Zhang X. Sensor bias fault detection and isolation in a class of nonlinear uncertain systems using adaptive estimation. *Automatic Control, IEEE Transactions on*. 2011; 56(5):1220–1226.

[17] Du M, Mhaskar P. Isolation and handling of sensor faults in nonlinear systems. *Automatica*. 2014;50(4):1066–1074.

[18] Du M, Scott J, Mhaskar P. Actuator and sensor fault isolation of nonlinear process systems. *Chemical Engineering Science*. 2013;104:294–303.

[19] Congalidis JP, Richards JR, Ray WH. Feedforward and feedback control of a solution copolymerization reactor. *AIChE Journal*. 1989;35(6):891–907.

[20] Mahmood M, Mhaskar P. Enhanced stability regions for model predictive control of nonlinear process systems. *AIChE journal*. 2008;54(6):1487–1498.

[21] Findeisen R, Imsland L, Allgöwer F, Foss BA. Output feedback stabilization of constrained systems with nonlinear predictive control. *Int J Rob & Non Contr*. 2003;13:211–227.

[22] Khalil HK. High-gain observers in nonlinear feedback control. In: *New directions in nonlinear observer design*, pp. 249–268. Springer. 1999;.

[23] Mahmood M, Gandhi R, Mhaskar P. Safe-Parking of Nonlinear Process Systems: Handling uncertainty and unavailability of measurements. *Chem Eng Sci*. 2008;63:5434 – 5446.

[24] Clark R. Instrument fault detection. *IEEE Transactions on Aerospace Electronic Systems*. 1978;14:456–465.

[25] Clark RN. A simplified instrument failure detection scheme. *Aerospace and Electronic Systems, IEEE Transactions on*. 1978;(4):558–563.

[26] Frank PM. Fault diagnosis in dynamic systems via state estimation-a survey. In: *System fault diagnostics, reliability and related knowledge-based approaches*, pp. 35–98. Springer. 1987;.

Appendix A:Lyapunov Based Model Predictive Control

Consider the nonlinear system of Eq. 4 with input constraints for which a control Lyapunov function V exists. Let Π denote a set of states where $\dot{V}(x(t))$ can be made negative by using the allowable values of the constrained input:

$$\Pi = \{x \in \mathbb{R}^n : sup L_f V(x) + inf L_G V(x) u \leq -\varepsilon^{**} V(x)\} \tag{17}$$

where $L_G V(x) = [L_{g_1} V(x), \ldots, L_{g_m} V(x)]$, with g_i the ith column of G and ε^{**} is a positive real number. The controller of [20] possesses a stability region, an estimate of which is given

by

$$\Omega = \{x \in \Pi : V(x) \leq c_{max}\}, \tag{18}$$

where c_{max} is a positive (preferably the largest possible) constant. Having defined the sets Π, Ω, the Lyapunov based predictive controller of [20] follows the formulation below:

$$u_{MPC}(x) := argmin\{J(x,t,u(.))|u(.) \in S\} \tag{19}$$

$$s.t. \quad \dot{x} = f(x) + G(x)u \tag{20}$$

$$L_G V(x(t))u(x(t)) \leq sup - L_f V(x(t)) - \varepsilon^{**} V(x(t)) \tag{21}$$

$$x(\tau) \in \Pi \quad \forall \tau \in [t, t+\Delta] \tag{22}$$

where $S = S(t,T)$ is the family of piecewise continuous functions (functions continuous from the right), with T denoting the control horizon, mapping $[t, t+T]$ into U. A control $u(.)$ in S is characterized by the sequence $\{u(t_k)\}$ and satisfies $u(\tau) = u(t_k)$ for all $\tau \in [t_k, t_k + \Delta]$. The objective function is given by

$$J(x,t,u(.)) = \int_t^{t+T} [\|x^u(s;x,t)\|^2_{Q_w} + \|u(s)\|^2_{R_w}]ds \tag{23}$$

where Q_w and R_w are positive semidefinite, and strictly positive definite, symmetric matrices, respectively, $x^u(s;x,t)$ denotes the solution of Eq. 20, due to control u, with initial state x at time t and T is specified horizon. In accordance with the receding horizon implementation, the minimizing control u_{MPC} is then applied to the system over $[t, t+\Delta]$, and the same procedure is repeated at the next instant. The stability property of the Lyapunov based predictive control design in [20] can be formulated as follows: given any positive real number d, there exists a positive real number Δ^* such that if $\Delta \in [0, \Delta^*]$ and $x(0) \in \Omega$ then $x(t) \in \Omega$, for all $t \geq 0$ and $\lim sup_{t\to\infty}\|x(t)\| \leq d$ (see e.g. [20] for further details). Note that the control design in Mahmood and Mhaskar (2008) is used only to illustrate the proposed framework

in this work and the obtained results hold under any control law that guarantees stability of the closed loop system.

List of Tables

List of Figures

Table 1: Process parameters for the solution copolymerization example.

Parameter	Value	Unit	Parameter	Value	Unit
V	1	m^3	A_{xba}	5.257×10^4	m^3/kmol·s
R	8.314	kJ/kmol·K	A_{xbb}	1577	m^3/kmol·s
ρ	8.79×10^2	kg/m^3	A_{xbs}	1514	m^3/kmol·s
c_p	2.01	kJ/kg·K	A_{xbt}	4.163×10^5	m^3/kmol·s
U	6.0×10^{-2}	kJ/m^2·s·K	E_i	1.25×10^5	kJ/kmol
A	4.6	m^2	E_{caa}	2.69×10^4	kJ/kmol
T_0	353.15	K	E_{cbb}	4.00×10^3	kJ/kmol
ε	1		E_{daa}	0.0	kJ/kmol
M_a	100.12	kg/kmol	E_{dbb}	0.0	kJ/kmol
M_b	86.09	kg/kmol	E_{paa}	2.42×10^4	kJ/kmol
M_i	164.21	kg/kmol	E_{pab}	2.42×10^4	kJ/kmol
M_s	78.11	kg/kmol	E_{pba}	1.80×10^4	kJ/kmol
M_t	44.05	kg/kmol	E_{pbb}	2.42×10^4	kJ/kmol
A_i	4.5×10^{14}	s^{-1}	E_{xaa}	2.42×10^4	kJ/kmol
A_{caa}	4.209×10^{11}	m^3/kmol·s	E_{xab}	2.42×10^4	kJ/kmol
A_{cbb}	1.61×10^9	m^3/kmol·s	E_{xas}	2.42×10^4	kJ/kmol
A_{daa}	0	m^3/kmol·s	E_{xat}	2.42×10^4	kJ/kmol
A_{dbb}	0	m^3/kmol·s	E_{xba}	1.80×10^4	kJ/kmol
A_{paa}	3.207×10^6	m^3/kmol·s	E_{xbb}	1.80×10^4	kJ/kmol

A_{pab}	1.233×10^5	m^3/kmol·s	E_{xbs}	1.80×10^4	kJ/kmol
A_{pba}	2.103×10^8	m^3/kmol·s	E_{xbt}	2.42×10^4	kJ/kmol
A_{pbb}	6.308×10^6	m^3/kmol·s	$-\Delta H_{paa}$	54.0×10^3	kJ/kmol
A_{xaa}	32.08	m^3/kmol·s	$-\Delta H_{pba}$	54.0×10^3	kJ/kmol
A_{xab}	1.234	m^3/kmol·s	$-\Delta H_{pab}$	86.0×10^3	kJ/kmol
A_{xas}	86.6	m^3/kmol·s	$-\Delta H_{pbb}$	86.0×10^3	kJ/kmol
A_{xat}	2085.0	m^3/kmol·s			

Table 2: Faults to which the residuals are insensitive and thresholds for the linear FDI filters.

Residual	Faults	Threshold	Residual	Faults	Threshold
r_1	$\tilde{y}_1$	0.3	r_2	$\tilde{y}_2$	6.3
r_3	$\tilde{y}_3$	0.55	r_4	$\tilde{y}_6$	0.55
r_5	$\tilde{y}_1, \tilde{y}_2$	0.18	r_6	$\tilde{y}_1, \tilde{y}_3$	0.18
r_7	$\tilde{y}_1, \tilde{y}_6$	0.18	r_8	$\tilde{y}_2, \tilde{y}_3$	0.55
r_9	$\tilde{y}_2, \tilde{y}_6$	0.5	r_{10}	$\tilde{y}_3, \tilde{y}_6$	0.5
r_{11}	$\tilde{u}_6$	0.5	r_{12}	$\tilde{u}_6, \tilde{y}_6$	0.5
r_{13}	$\tilde{u}_6, \tilde{y}_1$	0.01	r_{14}	$\tilde{u}_6, \tilde{y}_2$	0.5
r_{15}	$\tilde{u}_6, \tilde{y}_3$	0.5			

Table 3: Faults to which the residuals are insensitive and thresholds for the nonlinear FDI filters.

Residual	Faults	Threshold	Residual	Faults	Threshold
r_1	$\tilde{y}_1$	0.27	r_2	$\tilde{y}_2$	0.2
r_3	$\tilde{y}_3$	0.07	r_4	$\tilde{y}_6$	0.07
r_5	$\tilde{y}_1, \tilde{y}_2$	0.07	r_6	$\tilde{y}_1, \tilde{y}_3$	0.068
r_7	$\tilde{y}_1, \tilde{y}_6$	0.06	r_8	$\tilde{y}_2, \tilde{y}_3$	0.06
r_9	$\tilde{y}_2, \tilde{y}_6$	0.06	r_{10}	$\tilde{y}_3, \tilde{y}_6$	0.06
r_{11}	$\tilde{u}_6$	0.01	r_{12}	$\tilde{u}_6, \tilde{y}_6$	0.01
r_{13}	$\tilde{u}_6, \tilde{y}_1$	0.06	r_{14}	$\tilde{u}_6, \tilde{y}_2$	0.01
r_{15}	$\tilde{u}_6, \tilde{y}_3$	0.01			

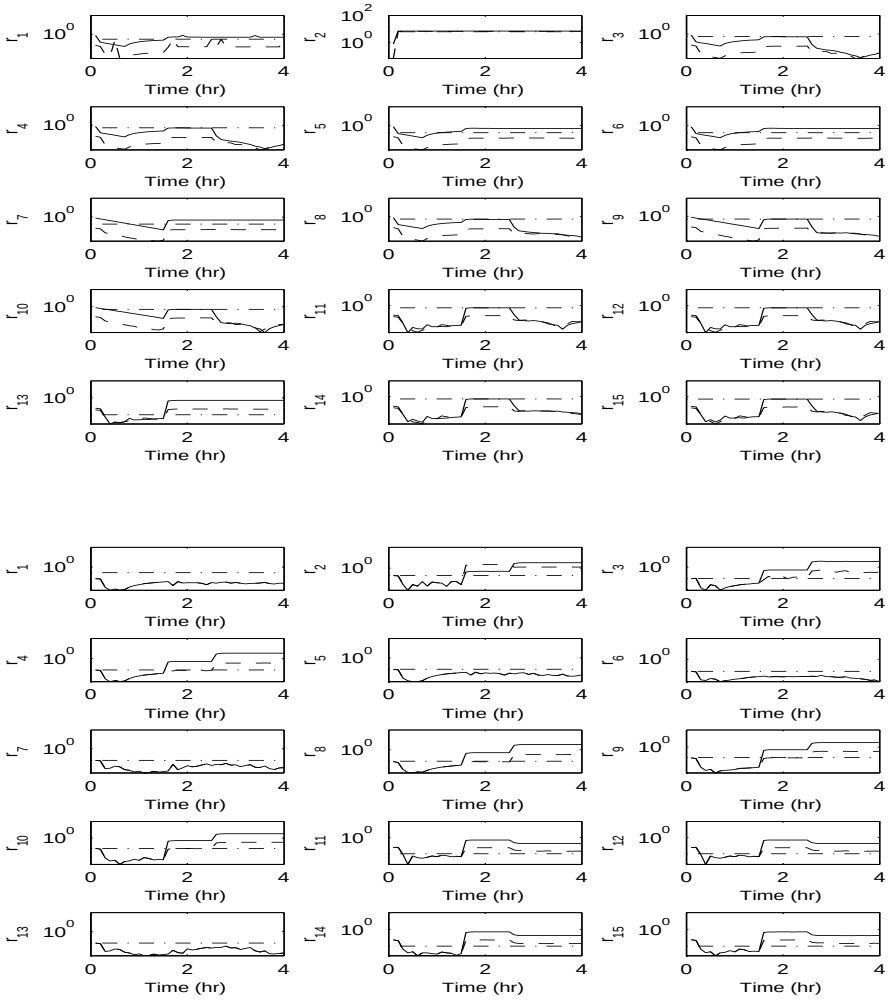

Figure 1: Evolution of the residuals for large (solid lines) and small (dashed-dotted lines) magnitude constant sensor fault. The thresholds are depicted by the dashed lines. Top: Using linear FDI filters enables FDI for the large sensor faults but only FD for small magnitude sensor fault. Bottom: Using nonlinear FDI filters enables FDI for both cases.

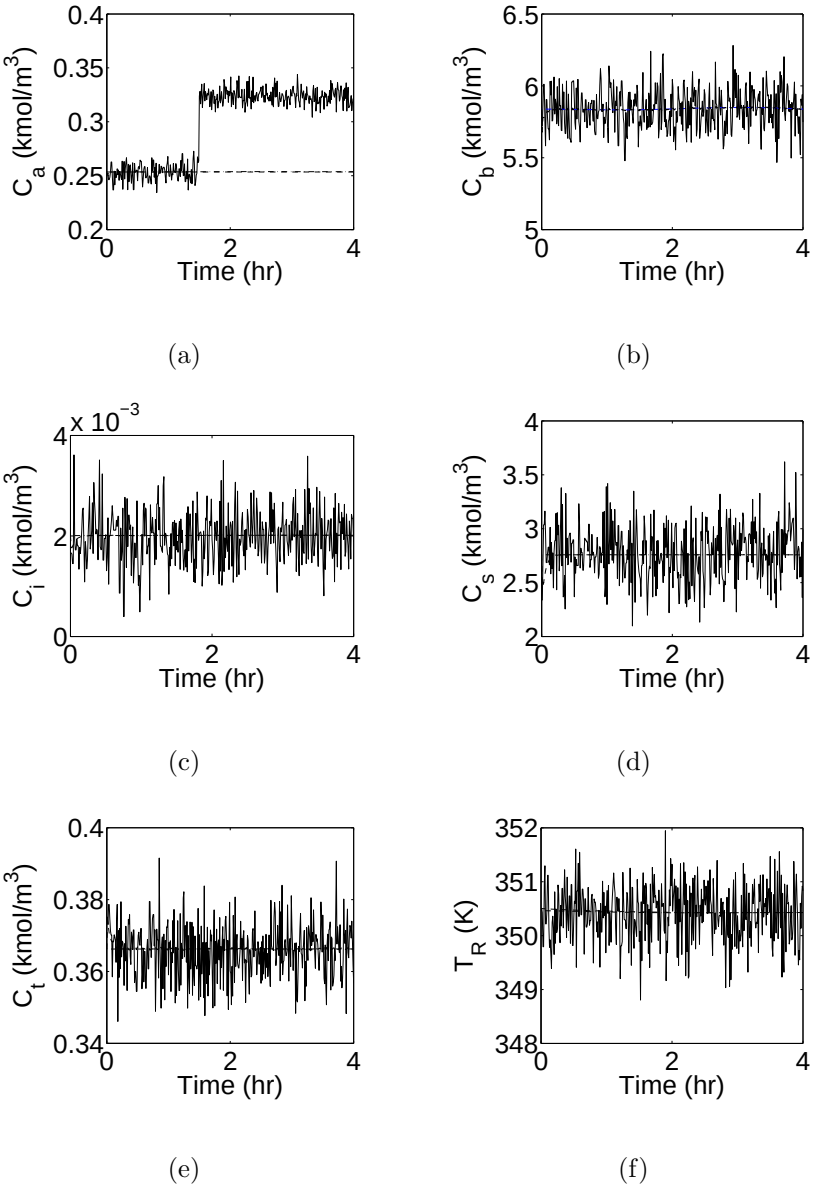

Figure 2: Evolution of the closed-loop measurements (solid lines), the state estimates (dashed lines), and the true values of the process states (dashed-dotted lines). A fault takes place in C_a sensor at time $t_r = 1.5$ hr and is handled. Since the observer does not use measurements of C_a, the state estimates stay close to their true values even after the fault takes place.

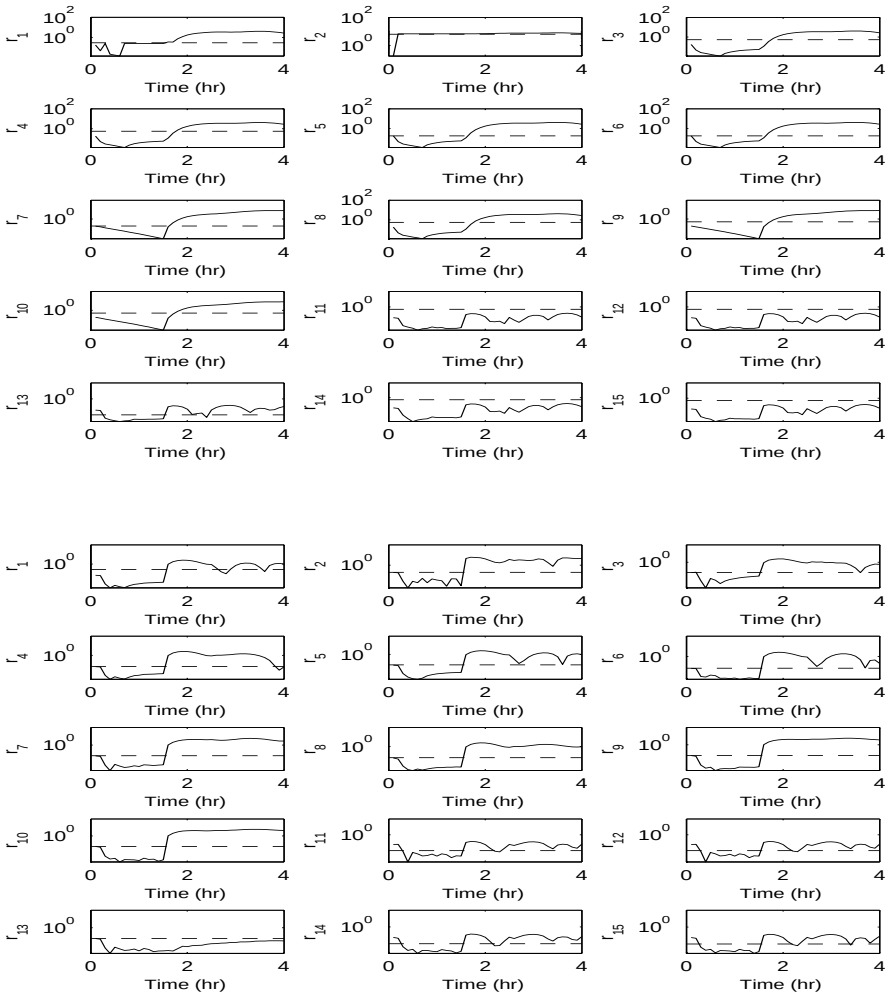

Figure 3: Evolution of the residuals (solid lines) and thresholds (dashed lines). Top: Using linear FDI filters: Since some of the residuals breach their thresholds, the fault is detected but is not isolated. Bottom: Using nonlinear FDI filters: Since all the residuals breach their thresholds except for r_{13}, which is insensitive to $\tilde{y}_1$ and $\tilde{u}_6$ (see Table 3), faults in y_1 and u_6 are isolated.

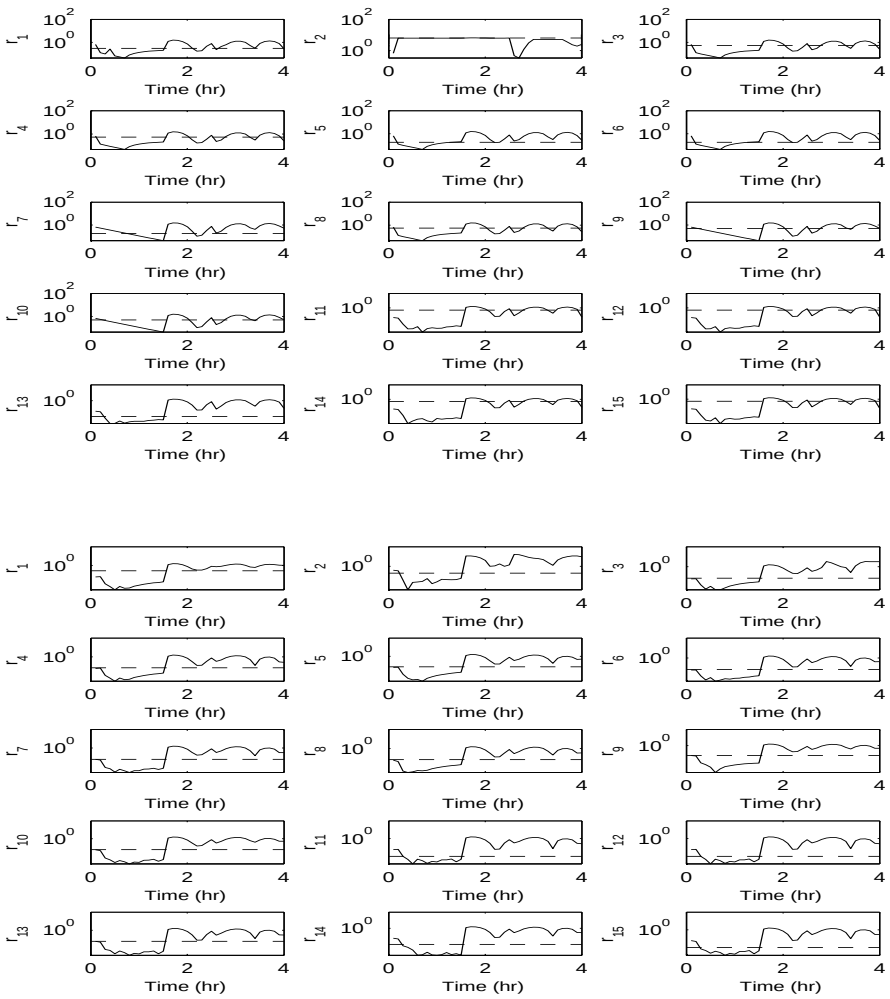

Figure 4: Evolution of the residuals (solid lines) and thresholds (dashed lines). Top: Using linear FDI filters, Bottom:Using nonlinear FDI filters. In both cases, since all the residuals breach their thresholds, the fault is detected but is not isolated.